LAWRENCE
LIVERMORE
NATIONAL
LABORATORY

LLNL-JRNL-560591

Black plasmons in metallic resonant cavities

M. Bora, T. Bond, E. Behymer, J. Britten

June 8, 2012

Applied physics letters

Disclaimer

Black plasmons in metallic resonant cavities

Mihail Bora, Elaine M. Behymer, Dietrich A. Dehlinger, Jerald A. Britten, Cindy C. Larson, Allan SP Chang, Keiko Munechika, Hoang T. Nguyen and Tiziana C. Bond**

AUTHOR ADDRESS

Lawrence Livermore National Laboratory, 7000 East Ave, Livermore, CA 94501

KEYWORDS

black plasmons, nanowire, broadband, absorbance, gold, silver, aluminum

ABSTRACT

We investigate a plasmonic resonant structure tunable from ultra-violet to near infrared wavelengths with maximum absorbance strength over 95% due to a highly efficient coupling with incident light. Additional harmonics are excited at higher frequencies extending the absorbance range to multiple wavelengths. We propose the concept of a 'black' plasmon resonator for which the modes are spaced arbitrarily close such that incident radiation is absorbed with high efficiency over the entire visible range.

Plasmons, electromagnetic waves propagating at metal dielectric interfaces[1], have a wide range of uses for refractive index based bio-sensing[2,3], molecular specific surface enhanced Raman spectroscopy (SERS)[4], improvement of photovoltaic efficiency[5], and plasmonic laser devices[6]. These applications require high extinction strength of the plasmonic resonances[7] such that near field effects dominate the physical behavior, hence design considerations for optimal structures aim at controlling both the resonant wavelength and the coupling with the incident light. Solar cell efficiency increases through conversion of evanescent plasmon field into excitons have been demonstrated, but these approaches have limited practicality because either they are effective only for narrow spectral and incidence angle ranges or rely on attenuated total internal reflection coupling geometry[2] which is often impractical . Nevertheless, recent studies that incorporate metallic nanostructures with strong coupling of incident light and broad spectral and angular coverage can provide a path for more efficient photovoltaics by means of plasmon-exciton conversion[8]. Herein we present a structure that addresses the broadband absorbance requirement for plasmonic photovoltaics.

Our concept of 'black plasmons' is inspired by previous work on 'black silicon'[9] and 'black silver'[10] substrates that have strong absorbance over the entire visible spectrum. For our substrates the broadband coverage is realized by designing a tunable plasmon cavity with multiple closely spaced resonances. The plasmonic substrate studied in this work is composed of a square array of vertical nanowires coated with gold, silver or aluminum and the visible averaged absorbance of the substrates can be increased above 75%, a remarkable feature considering that all three metals are used to fabricate highly reflective optical mirrors. The significance of aluminum nanostructures for large scale applications is underscored by the fact

that it is the least expensive pure metal and the third most abundant element in the Earth's crust after oxygen and silicon.

The nanowire array template is patterned using laser interference lithography and transferred into a silicon substrate using a directional deep reactive ion etching process with a mixture of sulfur hexafluoride (SF_6) for etching and perfluorocyclobutane (C_4F_8) for passivation[11]. The period of the array is 350 nm, chosen such that no diffraction grating effects take place in the visible spectrum under normal incidence. The height and profile of the nanowires is controlled by the etch time, the etchant composition and other parameters such as base pressure and bias power. Conditions for silicon etching in a SPTS Technologies instrument were set for 600 W plasma power, 25 sccm (standard cubic centimeters) of SF_6, 75 sccm for C_4F_8, base pressure of 20 mTorr, and bias power of 4 W. Further, the structure is sputtered with a conformal metallic film (Perkin Elmer) using a chromium adhesion layer for gold and no adhesion layer for silver and aluminum, due to the formation of a natural oxide layer that promotes growth of good quality films on silicon substrate. The sputtering conditions are set for 6 mT pressure, and 300-1000 W power. The height and diameter of the nanowires is determined by the etch time and sputtering time respectively (Figure 1a, b). Pairs of vertically aligned nanowires form a metal-dielectric-metal waveguide when the edge to edge separation is closer than 100 nm (Figure 1.c). Plasmon modes are excited by normal incident light waves in the transverse magnetic polarization mode.

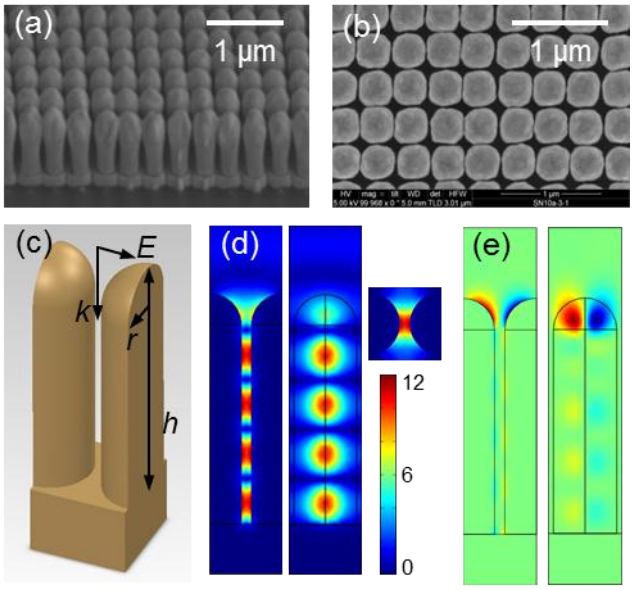

Figure 1. Scanning electron micrographs of the vertical metallic nanowires viewed from side (**a**) and top (**b**). **c**, Unit cell of the rectangular array centered on the plasmon nanocavity. The geometry of the array is specified by the pitch, radius and height of the nanowire array. Optical excitation of the cavity with normal incidence light polarized in the transverse magnetic mode **d,** Simulations of the electric field amplitude in the resonator seen from front, side and top. **e,** Nano-focusing in the plasmon cavity mode. Tangential power flow in the vertical symmetry planes of the cavity highlights the electromagnetic energy channeling into the inter-wire region from the top and the sides of the cavity.

The resonant modes of the cavity are formed by the interference of forward and backward propagating waves and are determined by the dispersion relation of the waveguide and the phase shifts at each end[12]:

$$2k_{sp}h + \varphi_1 + \varphi_2 = 2m\pi,$$

Where k_{sp} is the wavevector of the surface plasmon wave, h is the length of the cavity, φ_1 and φ_2, are the phase changes at the top and bottom boundaries and m is the resonance order. The

dispersion relation, $k_{sp}(\omega)$, can be approximated with that of a semi-infinite planar metal-dielectric-metal waveguide[13] or calculated analytically. Figure 1.d shows the electric field amplitude profile for a resonant mode of order m=4, as seen from three orthogonal cross sections. The node and anti-node conditions at each end correspond to phase shifts for $\varphi_1 = 0$ and $\varphi 2 = \pi$, however, depending on the waveguide geometry and dielectric medium they can be corrected to more accurate values. The simulations were carried on a unit cell composed of two half nanowires applying periodic boundary conditions along the unit vectors of the array, under normal incidence plane wave illumination, using a finite element method commercial software package (Comsol) distributed on a Linux cluster at Lawrence Livermore high performance computing facility.

Figure 1.e. highlights the power flow in the symmetry planes of the cavity corresponding to the vertical cross sections of the mode from Figure 1.d. A net power flow occurs only at the rounded top region such that the curved ending acts as a sub-wavelength electromagnetic lens. Utilizing a plasmon hybridization representation[14] the metal-dielectric-metal (MDM) plasmon can be decomposed in a symmetric linear combination of two single metal-dielectric (MD) interface plasmons. The electromagnetic bonding interaction between the two elementary MD states decreases the energy of the hybrid MDM plasmons. The lower energy of the symmetric MDM mode creates an electromagnetic potential well that confines the surface plasmon waves in a deep sub-wavelength volume[13]. The spherical ending of the nanowire is an effective coupler between the light and the plasmon modes, first because it allows for a large mode overlap between the two, and second because the gradual separation between the two metallic surfaces energetically favors focusing of the plasmon mode between the two nanowires. Although MD surface plasmon waves can be excited on individual nanowire alone when they are sufficiently

spaced apart, the absorbance is significantly higher for MDM plasmons[15], due to an increased field enhancement for the latter.

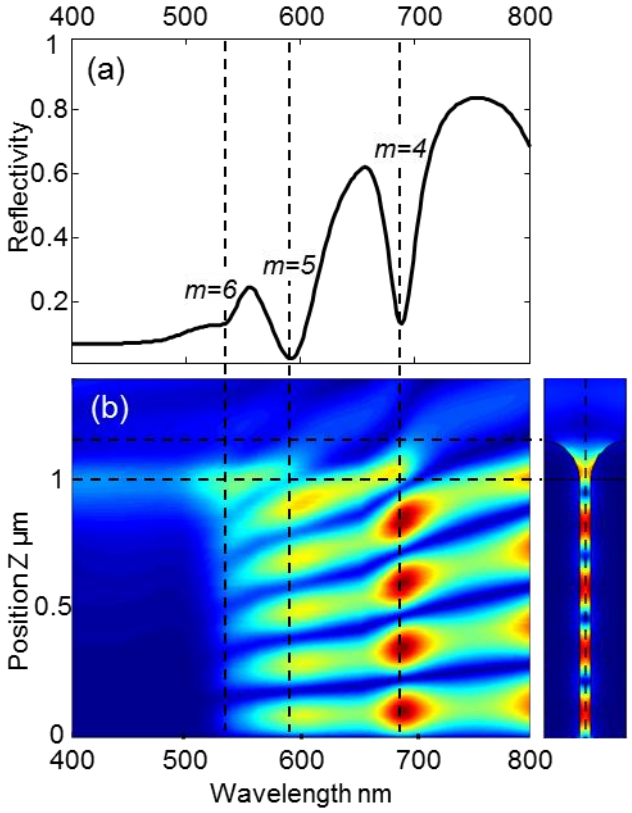

Figure 2. a, Simulations of normal incidence reflectance for a gold nano cavity 1150 nm long, 50 nm wide, showing resonances of order 5, 6, and 7 (from left to right) as reflectivity minima. **b**, Electric field amplitude simulation of the plasmon mode in the center of the cavity plotted as a function of position and excitation wavelength. Across the continuum of resonant modes, only the ones that have a large overlap with the incident photon modes are optically excited.

The frequency response of the resonator shows strong absorbance peaks that correspond to excitation of high electric field amplitude modes. The overall absorbance can be increased by adjusting the length of the resonator such that additional higher order modes are excited. Figure 2 represents the simulated measured reflectance of 350 nm pitch array made of gold nanowires of

300 nm diameter and 1150 nm height. The electric field amplitude profile of the mode on the vertical symmetry axis of the unit cell is plotted as a function of wavelength. The plasmon cavity resonates at all frequencies, however the strongest field enhancements are observed for the modes that extend further into the free space and have a better overlap with the incident photon field. Interestingly, weak plasmon modes are excited even for conditions that correspond to reflectivity maxima, suggesting that engineering the shape of the coupling end can lead to even stronger absorbance of the array over the whole spectrum.

The reflectivity was calculated for nanowires arrays of variable height made of three metals arranged in the increasing order of their bulk plasma frequency: gold (8.55 eV), silver (9.6 eV) and aluminum (15.3 eV)[16].

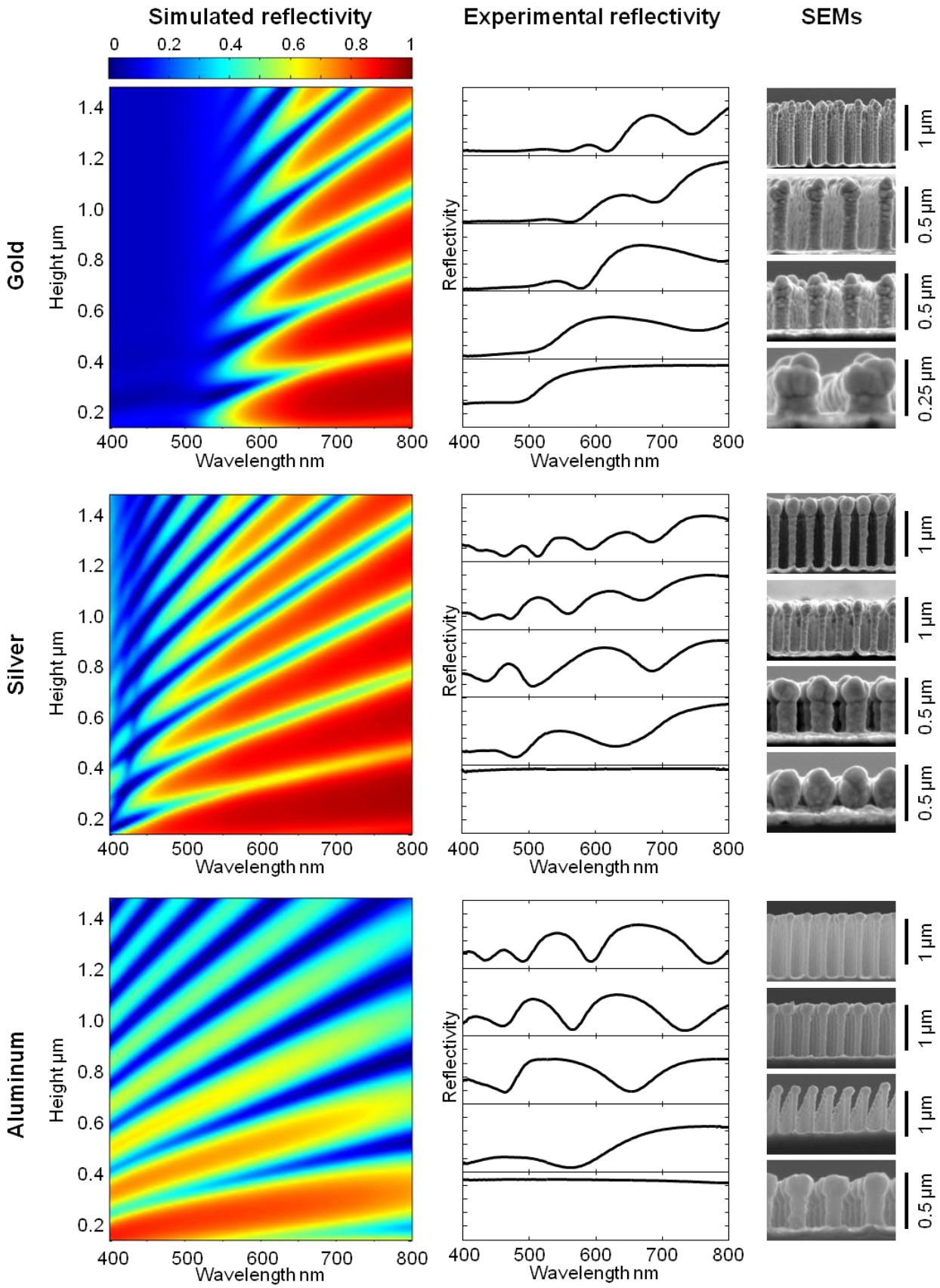
Simulated reflectivity
Experimental reflectivity
SEMs
0
0.2
0.4
0.6
0.8
1
Gold
Silver
Aluminum
Height µm
Reflectivity
Wavelength nm
400
500
600
700
800
0.2
0.4
0.6
0.8
1.0
1.2
1.4
1 µm
0.5 µm
0.25 µm

Figure 3. Simulations of the normal incidence reflected power for gold, silver and aluminum as a function of wavelength and nanowire height (color plot). Multiple resonances can be excited bellow the plasmon cutoff frequency. Experimental reflectivity for flat metallic films and nanowire arrays of increasing height, for gold, silver and aluminum are plotted alongside representative scanning electron micrographs cross sections. In all plots the reflectivity scale is 0 to 1.

In Figure 3 we show the simulated reflectance spectrum of 350 nm pitch array of vertical nanowires of 300 nm diameter, variable height h, and capped by a hemisphere of same diameter. At the lowest height the array is composed of hemispheres alone. The location of the resonances in the near infrared (~800 nm) is approximately the same for all the materials and geometry considered, since the dispersion of the plasmons in that region approaches the dispersion of light in air. In the case of gold only a fraction of the visible spectrum is covered by plasmon resonances as the cut off frequency corresponds to an excitation wavelength of 550 nm, while for silver and aluminum the entire visible spectrum is covered. As the height of the nanowire is increased the spacing between consecutive modes is decreasing enabling the cavity to have a strong absorbance at multiple excitation wavelengths.

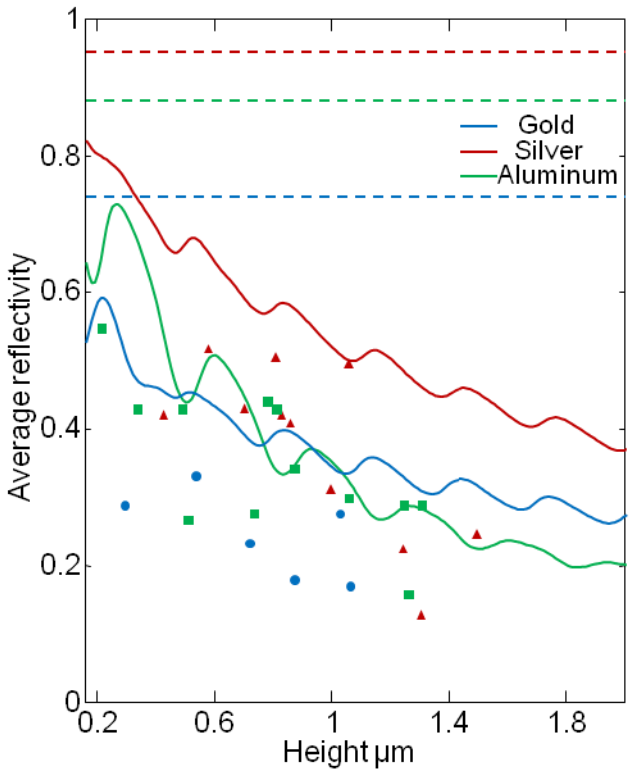

Figure 4. Simulated averaged visible reflectivity (400-800 nm) of an array of metallic nanowires as a function of the nanowire height for gold (red), silver (blue) and aluminum (green). The color coded dashed lines represent the average reflectivity for the flat metallic films, and the symbols are experimental measurements. A significant portion of the incident radiation is absorbed in plasmon resonant modes.

The effectiveness of the resonant array as a broadband absorber was assessed by calculating the average absorbance of the nanowire array in the 400-800 nm spectral range as a function of nanowire height (Figure 4). A stepwise decrease in reflectance is observed each time an additional resonance is added to the reflectance spectrum of the array. The absorbance of the array is referenced to the measured average reflectivity for flat films: 74% for gold, 95% for silver and 88% for aluminum. Experimental data points for fabricated samples are superimposed on the absorbance plot. The discrepancy between simulation and experiment arises mainly from

the difficulty to fabricate straight posts using a metal sputtering process. In this case the deposition rate at the top of the nanowire is larger than that at the bottom due to a shadowing effect of neighboring posts. We compensated for this effect by developing a silicon etching process that produces nanowire templates of a tapered shape with smaller diameter at the top.

In conclusion, we demonstrated multi-resonant plasmonic nanocavities in vertical metallic nanowire arrays with strong overlap and coupling between incident light and the plasmon modes. The absorbance of nanostructured metallic surfaces has been engineered to cover multiple wavelengths by increasing the longitudinal dimensions of the plasmon resonant nano-cavities. For large cavity sizes, beyond 3 μm for aluminum and longer for silver and gold (data not shown), the benefit of multiple resonances is offset by the weaker coupling into plasmons as the round trip losses in the cavity become significant enough to decrease the electric field amplitude of the modes. Using geometry dependent tuning, the resonances can be further optimized for renewable energy applications for a better overlap with the absorbance of semiconductor materials. Most of the incident light is reflected in the red side of the spectrum, as the resonance spacing is increased at longer wavelengths. The averaged absorbance becomes larger than the values calculated in Figure 4 when restricted to a frequency range above common semiconductor bandgaps and when weighted by the photon energy and the solar irradiance spectrum. If the refractive index of the inter-wire dielectric core is increased, the cutoff plasma frequency and the plasmon resonance locations are red shifted and the spacing between resonances becomes smaller as the optical length of resonator is increased. Based on these arguments, aluminum nanowire dielectric hybrid structures have a better spectral coverage than any other metal considered. Silver on the other hand has the lowest losses in the visible and it is most efficient for transferring energy from the plasmon modes into the absorptive dielectric

material while the gold nanowire arrays have a significant potential for biological sensing. Although in this study only gold, silver and aluminum materials were considered, the concept of enhancing material absorbance by engineering plasmon absorbance can be extended to other metals of interest. The high visible average absorbance characteristics of the vertical nanowire plasmonic array make it a potential candidate for realization of high efficiency photovoltaic devices.

AUTHOR INFORMATION

Corresponding Authors

* bora1@llnl.gov, bond7@llnl.gov

Funding Sources

This work was performed under the auspices of the U.S. Department of Energy by Lawrence Livermore National Laboratory under Contract DE-AC52-07NA27344. LLNLJRNL-425128.

REFERENCES

[1] H. F. Ghaemi, T. Thio, D. E. Grupp, T. W. Ebbesen, and H. J. Lezec, Phys. Rev. B **58** (11), 6779 (1998); W. L. Barnes, A. Dereux, and T. W. Ebbesen, Nature **424** (6950), 824 (2003).

[2] M. Bora, K. Celebi, J. Zuniga, C. Watson, K. M. Milaninia, and M. A. Baldo, Opt. Express **17** (1), 329 (2009).

[3] L. R. Hirsch, J. B. Jackson, A. Lee, N. J. Halas, and J. West, Anal. Chem. **75** (10), 2377 (2003); R. L. Rich and D. G. Myszka, J. Mol. Recognit. **24** (6), 892 (2011).

[4] A. S. P. Chang, M. Bora, H. T. Nguyen, E. M. Behymer, C. C. Larson, J. A. Britten, J. C. Carter, and T. C. Bond, in *Advanced Environmental, Chemical, and Biological Sensing Technologies Viii*, edited by T. VoDinh, R. A. Lieberman, and G. Gauglitz (Spie-Int Soc Optical Engineering, Bellingham, 2011), Vol. 8024; M. R. Gartia, Z. D. Xu, E. Behymer, H. Nguyen, J. A. Britten, C. Larson, R. Miles, M. Bora, A. S. P. Chang, T. C. Bond, and G. L. Liu, Nanotechnology **21** (39) (2010).

[5] A. J. Morfa, K. L. Rowlen, T. H. Reilly, M. J. Romero, and J. van de Lagemaat, Appl. Phys. Lett. **92** (1) (2008); V. E. Ferry, J. N. Munday, and H. A. Atwater, Adv. Mater. **22** (43), 4794 (2010); A. Polman and H. A. Atwater, Nat. Mater. **11** (3), 174 (2012).

[6] R. F. Oulton, V. J. Sorger, T. Zentgraf, R. M. Ma, C. Gladden, L. Dai, G. Bartal, and X. Zhang, Nature **461** (7264), 629 (2009); R. M. Ma, R. F. Oulton, V. J. Sorger, G. Bartal, and X. A. Zhang, Nat. Mater. **10** (2), 110 (2011).

[7] Fang Zheyu, Zhen Yu-Rong, Fan Linran, Zhu Xing, and P. Nordlander, Phys. Rev. B, Condens. Matter Mater. Phys. **85** (24), 245401 (7 pp.) (2012).

[8] N. S. King, Y. Li, C. Ayala-Orozco, T. Brannan, P. Nordlander, and N. J. Halas, ACS Nano **5** (9), 7254 (2011).

[9] T. H. Her, R. J. Finlay, C. Wu, S. Deliwala, and E. Mazur, Appl. Phys. Lett. **73** (12), 1673 (1998).

[10] Z. D. Xu, Y. Chen, M. R. Gartia, J. Jiang, and G. L. Liu, Appl. Phys. Lett. **98** (24) (2011).

[11] Y. J. Hung, S. L. Lee, B. J. Thibeault, and L. A. Coldren, IEEE J. Sel. Top. Quantum Electron. **17** (4), 869 (2011).

[12] R. de Waele, S. P. Burgos, H. A. Atwater, and A. Polman, Opt. Express **18** (12), 12770 (2010); R. de Waele, S. P. Burgos, A. Polman, and H. A. Atwater, Nano Lett. **9** (8), 2832 (2009); Z. P. Li, S. P. Zhang, N. J. Halas, P. Nordlander, and H. X. Xu, Small **7** (5), 593 (2011); M. W. Knight, N. K. Grady, R. Bardhan, F. Hao, P. Nordlander, and N. J. Halas, Nano Lett. **7** (8), 2346 (2007).

[13] M. Bora, B. J. Fasenfest, E. M. Behymer, A. S. P. Chang, H. T. Nguyen, J. A. Britten, C. C. Larson, J. W. Chan, R. R. Miles, and T. C. Bond, Nano Lett. **10** (8), 2832 (2010).

[14] E. Prodan, C. Radloff, N. J. Halas, and P. Nordlander, Science **302** (5644), 419 (2003).

[15] H. Ditlbacher, A. Hohenau, D. Wagner, U. Kreibig, M. Rogers, F. Hofer, F. R. Aussenegg, and J. R. Krenn, Phys. Rev. Lett. **95** (25) (2005); A. Manjavacas and F. J. G. de Abajo, Nano Lett. **9** (4), 1285 (2009); J. A. Dionne, L. A. Sweatlock, H. A. Atwater, and A. Polman, Phys. Rev. B **73** (3) (2006).

[16] Edward D. Palik, (1998).